




## ORIGINAL ARTICLE

# Pre-viking Swedish hillfort glass: A prospective long-term alteration analogue for vitrified nuclear waste

Jamie L. Weaver<sup>1,2</sup>  | Carolyn I. Pearce<sup>2</sup> | Rolf Sjöblom<sup>3</sup> | John S. McCloy<sup>2,4</sup>  |  
Micah Miller<sup>2</sup> | Tamas Varga<sup>2</sup>  | Bruce W. Arey<sup>2</sup> | Michele A. Conroy<sup>2</sup> |  
David K. Peeler<sup>2</sup> | Robert J. Koestler<sup>5</sup> | Paula T. DePriest<sup>5</sup> | Edward P. Vicenzi<sup>5</sup> |  
Eva Hjärthner-Holder<sup>6</sup> | Erik Ogenhall<sup>6</sup> | Albert A. Kruger<sup>7</sup>

<sup>1</sup>National Institute of Standards and Technology, Gaithersburg, MD, USA

<sup>2</sup>Pacific Northwest National Laboratory, Richland, WA, USA

<sup>3</sup>Luleå University of Technology, Luleå, Sweden

<sup>4</sup>School of Materials and Mechanical Engineering, Washington State University, Pullman, WA, USA

<sup>5</sup>Museum Conservation Institute, Smithsonian Institution, Suitland, MD, USA

<sup>6</sup>The Archaeologists, Geoarchaeological Laboratory, National Historical Museums (SHMM), Uppsala, Sweden

<sup>7</sup>U.S. Department of Energy, Office of River Protection, Richland, WA, USA

## Correspondence

Jamie L. Weaver

Email: jamie.weaver@nist.gov

and

Carolyn I. Pearce

Email: carolyn.pearce@pnnl.gov

## Funding information

U.S. Department of Energy, Grant/Award Number: 49141

## Abstract

Models for long-term glass alteration are required to satisfy performance predictions of vitrified nuclear waste in various disposal scenarios. Durability parameters are usually extracted from short-term laboratory tests, and sometimes checked with long-term natural experiments on glasses, termed analogues. In this paper, a unique potential ancient glass analogue from Sweden is discussed. The hillfort glass found at Broborg represents a unique case study as a vitrified waste glass analogue to compare to Low Activity Waste glass to be emplaced in near surface conditions at Hanford (USA). Glasses at Broborg have similar and dissimilar compositions to LAW glasses, allowing the testing of long-term alteration of different glass chemistries. In addition, the environmental history of the site is reasonably well documented. Initial investigations on previously collected samples established methodologies for handling and characterizing these artifacts by laboratory methods while preserving their alteration layers and cultural context. Evidence of possible biologically influenced glass alteration, and differential alteration in the 2 types of glass found at the Broborg site is presented.

## KEYWORDS

analogue, archeology, archeometry, corrosion, nuclear

## 1 | INTRODUCTION

An ongoing discussion in the field of glass durability is how to sufficiently validated short-term, laboratory experiment derived mechanisms for glass alteration, and how to extrapolate them to model long-term (tens of thousands to millions of years) glass alteration. This is a particularly poignant issue for the disposal of vitrified nuclear waste.<sup>1-3</sup> One suggested path is to test the models against analogue

glasses.<sup>4-7</sup> An analogue glass, and the environment in which it has been altered, should be as similar as possible to a glass whose durability is being assessed.<sup>3,8,9</sup> The analogue glass should be similar in composition (glass structure and chemistry), altering conditions (altering solution temperature, pH, flow rate and chemistry), and geometric parameters (surface area to volume ratio).<sup>10</sup> Additionally, the analogue glass should have been altered for an extended period of time as the rate of glass alteration, and

the mechanisms which dictate that rate, change with time.<sup>2,11</sup> A robust glass durability model should be able to describe the observed alteration behavior at long times for a variety of compositions and alteration environments. This, however, is a challenge to existing models, and more glass analogues are needed to refine the models.

A number of analogue glasses have been identified over the last half-century including volcanic glasses,<sup>5,8,12</sup> medieval glasses,<sup>6,13</sup> and Roman glasses.<sup>10,14-16</sup> In all cases, the analogue(s) under study were not compositionally identical to the glass being assessed, but they did contain most major elements (alkali, Si, Al, Fe, etc.), or elements that perform similar structural roles. One element that has been notably lacking in ancient analogue glasses is boron, which is a significant component of most nuclear waste glasses. The absence of boron is not surprising as it has low abundance in the earth's crust, and soluble evaporitic borate minerals typically having been removed by weathering. In addition, borosilicate glass as an industrial product was not introduced until the late 19th century.<sup>17</sup> Boron plays an important role in the structure of silicate glass when present at an appreciable quantity.<sup>18</sup> Target concentrations for Hanford's Low Activity Waste (LAW) glasses is 4 wt% - 16 wt%, and it has been observed to effect glass durability.<sup>19</sup> Therefore, boron is an important element to account for when modeling the long-term durability of a glass.<sup>1</sup> However, analyzing glass alteration processes over long periods of time as a function of other network formers, such as Al, is of value to understanding the durability of LAW nuclear glasses, particularly when the concentrations of Si, and alkali elements are similar.<sup>1</sup>

Broborg hillfort glasses, anthropogenic glasses produced in the Iron Age as a result of rock melting, have been identified as possible analogues for LAW glasses to be produced at the Hanford Nuclear Site, Washington State (USA).<sup>3,20,21</sup> The LAW glasses will be disposed at the Hanford site in the near-surface Integrated Disposal Facility (IDF). Although the LAW waste package is glass surrounded by a stainless-steel container, the performance assessment for the IDF does not take the container into account. Rather, the assessment assumes direct contact between the LAW glass and the near surface environment.<sup>22</sup> The Broborg hillfort glasses have been identified as possibly analogues for LAW glass as they have been altered under near-surface conditions with the glass in contact with the surrounding soil.<sup>20</sup> This article covers the initial analyses and assessment of utilizing the vitrified materials from the 1500-year-old Broborg hillfort as a long-term alteration analogue for Hanford LAW glasses.

In addition to being prospective analogue glasses, the Broborg hillfort glasses are examples of early Scandinavian glassmaking technology, and are artifacts of interest to historical and archeological communities. In review of the

literature for the analysis and assessment of analogue glasses it was found that there was no specific procedure for the analysis of a historically important analogue glass. To address this gap a novel procedure has been designed to extract relevant alteration data while maintaining the physical stability of the artifact so that it could be preserved for future research. This method has been created by glass scientists working in concert with those specializing in humanistic studies (art history, history, and archeology) and conservation sciences. It is designed to produce data that could be used to validate current glass alteration models, and to provide historical insight into the production and purpose of the artifacts under study.

In summary, the goals of the presented research are to (i) evaluate the use of Broborg glasses as analogues for the long-term alteration of Hanford nuclear waste glass, (ii) to develop artifact sampling and analysis techniques that allow for the preservation of the main body of the artifacts for future study, (iii) gain insight into ancient Scandinavian hillfort building methods. The research presented in this text is the first stage in the hillfort analogue glass research project, primarily focused on goals (i) and (ii), and is one in a series of papers on this project. A full overview of the project has been previously detailed by Sjoblom et al.<sup>21</sup>

## 2 | BACKGROUND

### 2.1 | Vitrified hillforts

A hillfort is a structure used as a fortified refuge, lookout, trading post or defended settlement.<sup>23</sup> Early papers on Swedish hillforts have connected the construction of these forts to war and military defense.<sup>24,25</sup> Olausson suggested that the primary function of these hillforts may not have been strictly related to fortification, but rather they served as a connection between towns and aided in the centralization and production of political power in pre-Viking Scandinavia.<sup>26</sup> Alternatively, Wall has proposed that the walls were built as a cultic exercise to provide visual separation between the living world and the inaccessible world.<sup>27</sup>

Hillforts are typically found in Western Europe, and often follow the contours of a hill.<sup>27</sup> They consist of one or more lines of earthworks, stockades, or defensive walls, and are sometimes surrounded by external ditches. Most are constructed with dry stone wall technology, although more than 100 European hillforts have been found which are partially vitrified. There is still much controversy over why and how this vitrification occurred,<sup>28</sup> but several studies have suggested that sections of the forts were intentionally vitrified to reinforce the stone walls; similar to how mortar is applied to brick walls to add structural strength.<sup>29</sup> Kresten has asserted in his study of Broborg glasses that the temperature required for vitrification would have been

too high to be achieved by chance.<sup>30</sup> He had determined that the required temperature to vitrify the stones is around 1200°C.<sup>30</sup>

The walls of Broborg are not of a water-tight construction, and include voids between stones. These voids could have been part of the design; developed due to the fire-cracking of the stone during heating, or the result of settling of the structure overtime. These voids have either been intentionally or naturally backfilled with soil, and inorganic and organic debris. Some of the vitrified material is also porous, and the pores are open and sometimes interconnected (example in Figure 1C). The open nature of the wall has allowed water to flow through its structure and into the underlying hill.

## 2.2 | Environmental history of broborg

For glass analogues to be useful for validating modeling the alteration influencing environmental conditions must be known. Information on the paleogeography, vegetation changes, and human impact on the area surrounding

Broborg (Husby-Långhundra Parish) is available because the region is of archaeological importance with respect to the early history of Swedish/Scandinavian iron working.<sup>31</sup> From historical records it is known that Broborg was probably in use for at least some time during the Swedish Migration period (375-550 C.E.), but was abandoned at least a millennium ago.<sup>30</sup> The land has been rising as part of a geological rebound that has taken place since the end of the Ice Age, resulting in drying of the water-way at the bottom of the Broborg hill.<sup>31</sup> The development of the surrounding countryside is known from pollen analyses of cores from nearby sediments.<sup>32,33</sup> This includes the disappearance of certain near-by lakes together with increased use of land for agricultural purposes and some deforestation. Paper meteorological records for the region date back to the 17<sup>th</sup> century.<sup>34</sup> These documents include detailed information on the past climate of the area with a temporal resolution of daily values and, more commonly, monthly averages. The longest running recorded metrological data for this area was started in 1722, and this data continues to be recorded to today.<sup>34</sup> In general, the near-field chemistry

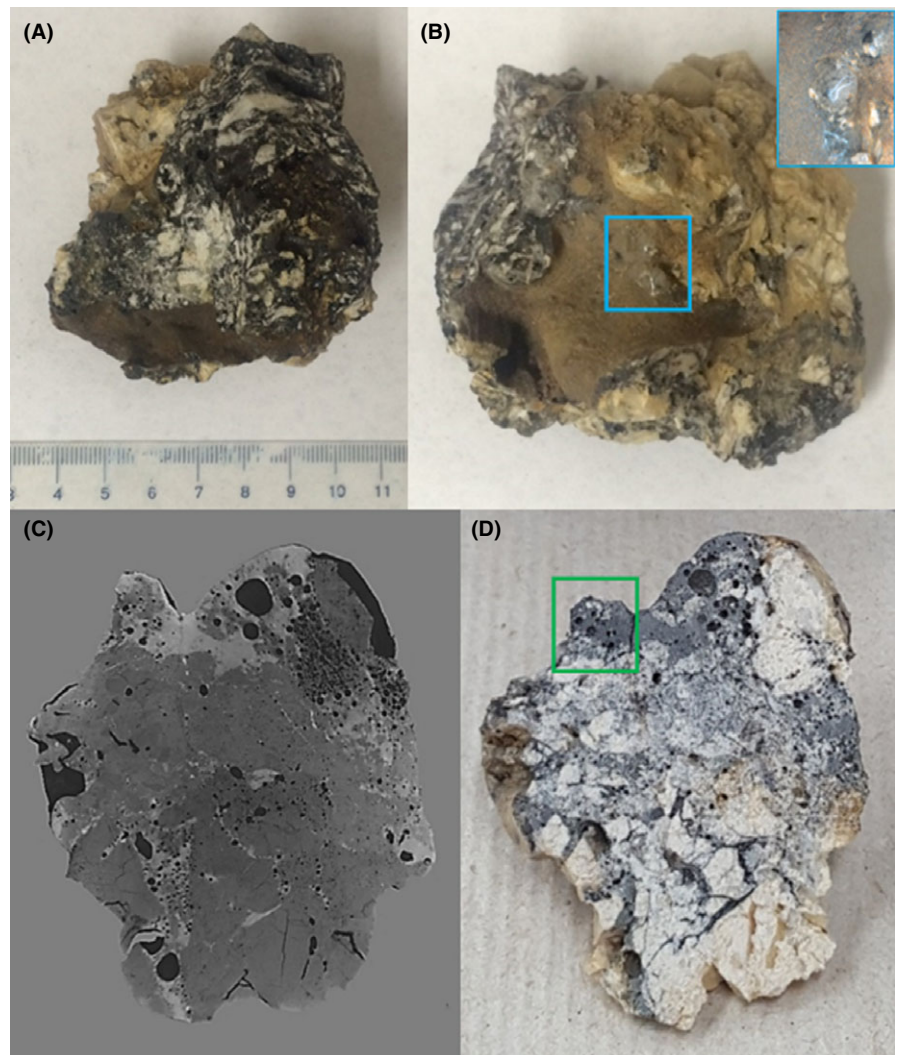


**FIGURE 1** Back (A) and front (B) image of the sample from Broborg (inset in B shows higher magnification image of the clear glass), X-ray computed tomography image of plane selected for sectioning (C) and image of cut surface after sectioning (D). Green box represents area selected for high resolution  $\mu$ XRF mapping

affecting the glass in the wall has been governed by the initial conditions after the firing, with most of the influencing parameters (such as temperature, water volume) external to the glass following global climate trends over the last 1500 years. These conditions have been described by Moberg et al.<sup>35</sup> and can be corroborated by the metrological records that are held within the Swedish archives.<sup>34</sup>

### 2.3 | Broborg hillfort glass

The hillfort sample analyzed in this study was collected with other specimens from the Broborg site near Uppsala Sweden (Husby-Långhundra Parish, Uppland; 662818N, 162066E) by Kresten and co-workers in the early 1990s, and have been previously described in detail.<sup>28,30,36</sup> The archeological samples are  $\approx 5 \text{ cm}^3$  to  $\approx 30 \text{ cm}^3$  in size, and date from between 650 C.E. to 1050 C.E.<sup>36</sup> Lithologically, they are made up of local granitic gneiss boulders, bound together by glassy regions. These glassy volumes are reported to represent the residue of partly melted amphibolite rock.<sup>30,36</sup> An amphibolite is a metamorphic rock composed mainly of amphibole minerals, plagioclase feldspar, and quartz.<sup>37</sup> An amphibole mineral is a double chain silicate in which the chains are variably arranged. An example of an amphibole mineral is actinolite.<sup>37</sup>

The specimen selected for analysis in this study contained 2 types of glass, one dark and one clear, which were originally identified and characterized by Kresten et al.<sup>28,36</sup> The darker glass has been proposed to have formed due to incongruent melting of amphibolite,<sup>30</sup> and has a reported composition similar to basaltic glasses: high in iron and low in alkali elements. Kresten suggested that iron-containing crystals present in the dark glass could have formed upon cooling, or were present in the initial rocks which underwent incomplete melting during the firing of the wall.<sup>30</sup> The second glass, referred to as the clear glass, is a quartz-feldspathic glass, and could have formed by the melting and pooling of phases present in the granite gneiss boulders used to form the wall.<sup>30</sup> Evidence of charcoal at the Broborg site, along with charcoal imprints on the molten surfaces, suggest that wood fire could have been used as a heat source for the melting of these glasses. Some Broborg glass samples have been previously found to have inclusions of Fe metal, suggesting that the melts were produced under reducing conditions.<sup>36</sup>

## 3 | EXPERIMENTAL PROCEDURES

### 3.1 | Criteria for assessment of a glass as an analogue

In general, and as previously stated by others,<sup>1,3,6,8,9</sup> for glasses to be suitable analogues for vitrified nuclear waste

glasses they need to meet the following criteria: (i) be of similar chemical composition, or contain elements that played similar structural roles as those present in the glass of interest, (ii) show physical and chemical indications of alteration (hydrated alteration layer(s), secondary alteration products), (iii) have been altered under similar conditions to those expected for the glasses of interest, and (iv) have known provenance to ensure the alteration layers were not disturbed nor removed during or after sample excavation. This study assesses the validity of the 2 types of Broborg glasses as analogues for LAW glasses following these criteria.

### 3.2 | Handling, documentation, and order of analyses

A new sample preparation and handling method was designed with the aid of Museum Conservation Institute (Smithsonian Institution, USA), and Geoarkeologiskt Laboratorium, Arkeologerna, Statens Historiska Museer, (Geoarchaeological Laboratory, The Archaeologists, National Historical Museums, Uppsala, Sweden), allow for the extraction of relevant alteration data while maintaining the historical integrity of the Broborg hillfort glass artifacts. Upon acquisition all samples were visually inspected and their physical appearance documented, both in written and digital photographic formats, before any sectioning occurred. The artifact selected for sectioning and detailed analysis contained both clear and dark glasses on its surface, and was physically robust enough to undergo: (i) X-ray computed tomography (XCT) to assess internal structure and define key regions of interest for sectioning, (ii) dry cutting with a band saw, and (iii) subsequent analysis by micro X-ray diffraction ( $\mu$ -XRD), micro X-ray fluorescence ( $\mu$ -XRF), scanning electron microscopy (SEM), focused ion beam (FIB) sectioning, and scanning transmission electron microscopy (STEM). A top-down approach was implemented regarding these analyses; beginning with nondestructive characterization techniques, followed by semidestructive and lastly destructive analyses. In some cases it was necessary to remove smaller samples from the sectioned material in order to meet analysis instrument sample size limitations.

### 3.3 | X-ray computed tomography (XCT, nondestructive)

The internal microstructure of the sample prior to sectioning was analyzed by XCT. The sample was scanned with a Nikon XTH 320/225 kV high-resolution microfocus tomography scanner (Nikon Metrology, Brighton, MI, USA) at 95 kV and 165  $\mu$ A X-ray power for optimum image quality and contrast. The sample was rotated continuously during the scans with momentary stops to collect each projection (shuttling mode) to minimize ring artifacts.



A total of 3142 projections were collected over 360° with 708 ms exposure time and 4 frames per projection. Image voxel size was 38  $\mu\text{m}^3$ . The images were reconstructed to obtain a 3-dimensional dataset with CT Pro 3D (Metris XT 2.2, Nikon Metrology). The representative slice tomography image shown in Figure 1A-D compared to the photograph was created using the visualization program VG Studio Max 2.1 (Volume Graphics GmbH, Germany).

### 3.4 | Sectioning (semidestructive)

Sectioning was necessary to produce samples suitable for subsequent analyses. The specimen was sectioned only after it had been determined that it would not fracture or crumble during cutting. A key consideration for the sectioning process was to prevent contamination of the artifact (both the part to be analyzed and the part to be preserved) with carbon-rich material such as an oil or graphite based lubricant. Such contamination would have made it difficult to analyze the organic material on the sample surface. In addition, water-based lubricants were avoided since they might negatively impact the delicate alteration structures, and might remove soil/organic deposits. Therefore, no solid or liquid lubricants were used during sectioning. A dry cutting procedure was used, with a Metal Mizer Model 2018 band saw, a pressure driven blade, and air cooling directed onto the blade. A new Ni-coated, 410 stainless steel blade with an electroplated diamond abrasive of grit size 35/40 (Greenlee Diamond Tool Company) was used for sectioning. All materials were held in place by Teflon-lined clamps during the cutting. The dry cutting procedure was evaluated by conducting a test cut on a similar sized granite material prior to the cutting of the Broborg sample. This test allowed for the determination of cutting temperature, quality of the cut, and potential for contamination by the blade. During the test cut the granite remained cool to touch, and the cut surface was visually smooth. The XRF analysis of the cut surface showed no evidence of transfer of Ni-rich blade material to the test sample. The cutting blade was cleaned with ethanol and fully dried between cutting the test sample and the Broborg sample to avoid cross-contamination between the materials.

The location for sectioning of the Broborg sample was determined by visual inspection of the surface coupled with contrast patterns in XCT (Figure 1C). The area to be cut: (i) had regions of different density (clear and dark regions in the XCT image, suggesting differences in elemental chemistry), (ii) contained regions that had melted (based on the presence of observable bubble structure), and (iii) had visible dark and clear glassy materials on the surface. The cut sites were assessed for robustness by first completing a small test cut at the edge of the sample, and throughout the cutting process the sample was carefully visually monitored to ensure that the artifact was not exposed to extreme

torsion. The Broborg sample was cut in a single pass, and any materials loosened from the surface of the sample were collected, labeled, and stored for future analysis. Subsectioning of the removed section was completed by a dry and unlubricated Isomet slow speed saw (Buehler), with a 22.86 cm blade that was identical in chemistry and grit to the blade utilized for the bandsaw cut (Greenlee Diamond Tool Company).

### 3.5 | Micro X-ray diffraction ( $\mu\text{XRD}$ , nondestructive)

Samples taken from the original specimen were characterized with a Rigaku D/Max Rapid II  $\mu\text{XRD}$  instrument with an image plate detector. X-rays were produced with a MicroMax 007HF generator fitted with a rotating Cr anode ( $\lambda = 0.22897$  nm) and focused on the specimen through a 300  $\mu\text{m}$  diameter collimator. The 2DP, Rigaku 2D Data Processing Software (Ver. 1.0, Rigaku, 2007) was used to integrate the diffraction rings captured by the detector. The analysis of diffraction data was carried out with JADE 8.5 from Materials Data Inc., and the PDF4+ database from the Inorganic Crystal Structure Database (ICSD).

### 3.6 | Micro-X-Ray fluorescence ( $\mu\text{XRF}$ , nondestructive)

The  $\mu\text{XRF}$  analyses were performed with an EDAX Orbis Micro-XRF Analyzer with a Mo X-ray source and a silicon drift detector. Elemental data were collected under vacuum with a 45 kVp polychromatic beam focused to 30  $\mu\text{m}$  using a polycapillary optic. The full samples were mapped with a 1 mm spot size, and the partial view was mapped using the polycapillary optic. The raw images are shown in Figure 2. A fluorescence spectrum from 0 keV to 40 keV was collected at each location, and this allowed for the reliable detection of Na and heavier elements ( $Z > 11$ ). Quantification of spectra at specific locations was performed with peak to peak ratios, in lieu of elemental standards, following the procedure described by Shen et al.<sup>38</sup>

### 3.7 | Focused ion beam-scanning electron microscopy (FIB-SEM, semidestructive)

Samples were analyzed with a FEI Helios NanoLab 660 (Hillsboro, OR) FIB-SEM with an Energy Dispersive Spectrometer (EDS) (EDAX Newark, NJ). An accelerating voltage of 5-10 kV, and a working distance of 4 mm were used in the analyses. Imaging was performed with an Everhart-Thornley secondary electron (SE) detector in field-free conditions, and through-the-lens detectors (TLD) for SE and back-scatter electron (BSE) imaging in immersion mode. FIB-TEM samples were prepared with standard techniques

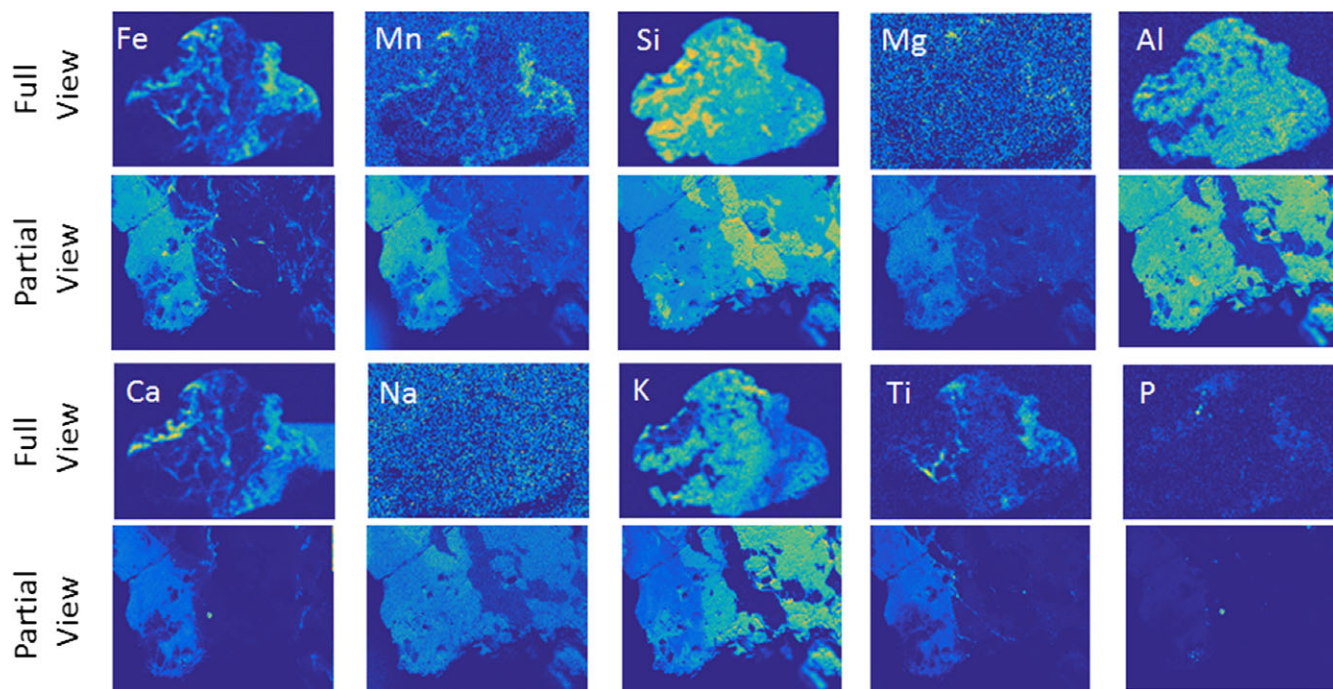


**FIGURE 2**  $\mu$ XRF raw intensity elemental maps of the Broborg sample. Full view (low resolution) and partial view (high resolution). The intensity of the color is linear and indicates the relative number of counts at the energy corresponding to a specific element. Color scale is normalized such that yellow and blue represents the highest and lowest x-ray intensities, respectively

for TEM liftouts. A voltage of 30 kV and currents of 21 nA and 2.5 nA were used to cut a trench in the material. The removed sample was then attached to a copper OmniProbe grid. The final thinning procedures used a voltage of 30 kV at a current of 400 pA with a final cleaning step with 5 kV and 2 kV at a current of 100 pA.

### 3.8 | Scanning transmission electron microscopy (STEM, nondestructive)

The FIB samples were analyzed with a JEOL ARM200F (JEOL, Peabody, MA) in scanning transmission electron microscope (STEM) mode operated at 200 keV and equipped with a Noran™ (Thermo Scientific, Waltham, MA) EDS system. Elemental mapping was performed with a 7  $\mu$ A emission current, spot size 8 C, and a 40  $\mu$ m aperture.

## 4 | RESULTS

### 4.1 | Visual and chemical description of sample

Dust and visible dirt covered most of the exteriors of the sample, and chisel marks, most likely incurred during the excavation process, were noted on some edges. The specimen selected for analysis in this study (Figure 1A, B) is from a region of the Broborg hillfort wall relatively close to the fort's historical entrance. Previous analyses of

samples from the same area of Broborg as the materials analyzed in this study (near, but not directly at the entrance of the fort) found that samples from this region are predominately composed of both the local granitic gneiss (cream or white colored, with black speckling) and the partly melted amphibolite (darker, amorphous gray or dark gray regions).<sup>30,36</sup> The exterior surfaces of the samples, both the one analyzed in this study and in Kresten's previous work, had clear glass and dark glass regions (Figure 1B).

The freshly cut face (Figure 1D) of the sample analyzed in this study shows that the interior is heterogeneous. The cream-colored material is interspersed with a vesiculated, gray material. X-ray diffraction of the gray areas show that they are amorphous (Figure 3A).  $\mu$ XRF maps and higher resolution  $\mu$ XRF images show that there are regions of high Si associated with cream colored areas (Table 1, area 2), and that the dark areas have less Si and higher relative concentrations of Fe, Mn, Mg, Ca, Na, K, and Ti (Table 1, area 1). The  $\mu$ XRD of the high Si areas show peaks indexed as crystalline quartz ( $\text{SiO}_2$ ), and a large amorphous background (Figure 3B). The  $\mu$ XRD of the dark regions show peak patterns consistent with quartz, oxides belonging to the spinel group (eg, magnetite [ $\text{Fe}^{2+}\text{Fe}_2^{3+}\text{O}_4$ ], hausmannite [ $\text{Mn}^{2+}\text{Mn}_2^{3+}\text{O}_4$ ] and magnesioferrite [ $\text{MgFe}_2^{3+}\text{O}_4$ ]), calcium rich plagioclase feldspar (eg, anorthite [ $\text{CaAl}_2\text{Si}_2\text{O}_8$ ]), and members of the pyroxene group (eg, diopside [ $\text{CaMgSi}_2\text{O}_6$ ]), as well as a significant amorphous component (Figure 3A).

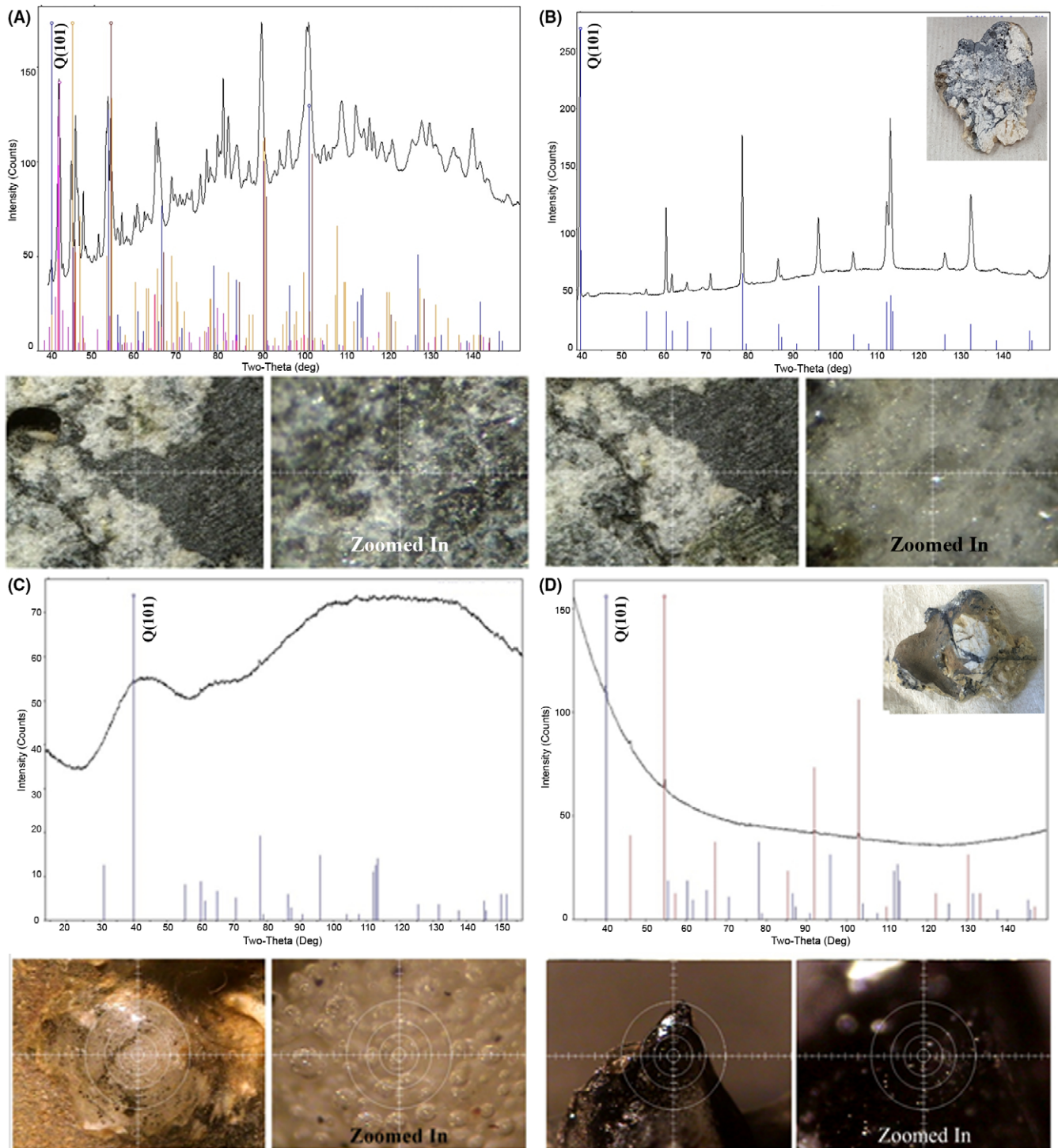


**FIGURE 3**  $\mu$ XRD patterns from 4 areas of the Broborg sample. A, is a mixed gray area of crystalline material with manganese oxide  $Mn_3O_4$  (dark blue), anorthite  $CaAl_2Si_2O_8$  (pink), quartz  $SiO_2$  (light blue), diopside  $CaMgSi_2O_6$  (yellow), and magnesioferrite  $MgFe_2O_4$  (dark red); B, is an area of crystalline quartz  $SiO_2$  (light blue) with amorphous material indicated by the high background and broad peaks; C, shows an amorphous area of clear glass (with minor peaks corresponding to quartz  $SiO_2$  [light blue]); and D shows an amorphous area of dark glass (with minor peaks corresponding to quartz  $SiO_2$  [light blue] and magnetite  $Fe_3O_4$  [black])

Many of these phases are consistent with those identified and discussed by Kresten et al.<sup>36</sup>

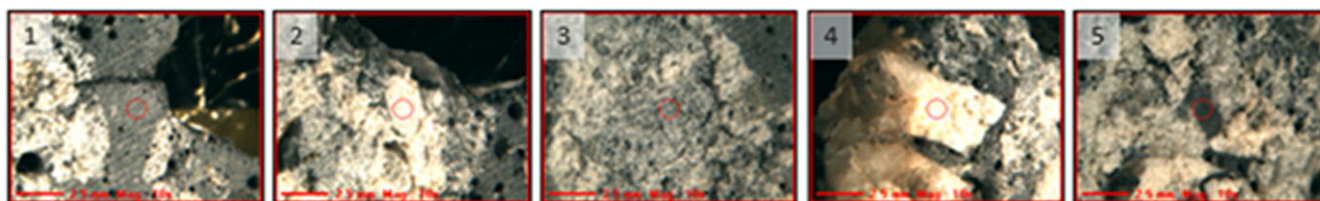
Small regions of clear and dark glasses were identified on the exterior surface of the sample (Figure 3C, D).

Optical microscopy of the clear glass reveals trapped bubbles (Figure 3C). SEM images of the area on and around both glasses show an intermittent surface layer of organic material (Figure 4A, B). Some of the organic material was



**TABLE 1** Elemental concentration of Broborg sample section determined by  $\mu$ XRF and reported in wt%. Images of locations where measurements were made are shown below (red circles). Quantification of spectra at specific locations was performed with peak to peak ratios, in lieu of elemental standards, following the procedure described by Shen et al.<sup>38</sup> This data was collected and analyzed at Pacific Northwest National Laboratory

Location Description of material	1 Mid Gray, not-mixed	2 Light, mixed	3 Mid Gray, mixed	4 Light, not-mixed	5 Dark Gray, possibly mixed
Na <sub>2</sub> O	4.52	2.78	2.76	1.13	2.86
MgO	2.55	0.42	0.5	0.37	1.17
Al <sub>2</sub> O <sub>3</sub>	13.44	6.19	13.13	1.49	12.65
SiO <sub>2</sub>	47.44	78.71	61.01	91.9	55.32
P <sub>2</sub> O <sub>5</sub>	1.87	0.16	0.13	0.8	0.56
SO <sub>3</sub>	4.19	3.95	6.58	2.37	5.53
K <sub>2</sub> O	2.26	7.12	13.35	0.56	9.4
CaO	10.73	0.21	0.69	0.95	5.56
TiO <sub>2</sub>	1.54	0.15	0.34	0.05	1.07
MnO	0.32	0.02	0.03	0.01	0.12
Fe <sub>2</sub> O <sub>3</sub>	11.13	0.29	1.5	0.37	5.75
Total	100	100	100	100	100



preliminarily identified as spores, lichens, and fungal hyphae. Additional analyses of the biological material are currently underway.

The  $\mu$ XRD of the glassy regions show they are indeed predominantly amorphous, with a very minor crystalline component (Figure 3C,D). The  $\mu$ XRF results, detailed in Table 2, show that the bulk of the clear glass is rich in Si, Al, and K, with small concentrations of Mg and Ca, and contains much less Fe than the gray areas of the sample and the dark glass. In addition to significantly higher amounts of Fe, the dark glass was also significantly lower in alkali and Si, had more Ca, and contained a similar amount of Al to the clear glass. The elemental composition of the glasses estimated with  $\mu$ XRF are within a few wt% of that previously obtained by Kresten for all oxides except SiO<sub>2</sub> and Al<sub>2</sub>O<sub>3</sub>.<sup>30</sup> The clear glass area analyzed in this study had a lower Al<sub>2</sub>O<sub>3</sub> and a higher SiO<sub>2</sub> content compared with the sample analyzed previously by Kresten.<sup>36</sup>

## 4.2 | Glass alteration

The FIB cross-sections removed from the clear glass (Figure 4C) were analyzed with STEM-EDS to determine whether an alteration layer was present on the surface of the

clear glass (Figure 5). From the FIB sections it was found that the surface of the glass consistently contained concentric half-ring alteration patterns that penetrated  $\approx 0.25 \mu\text{m}$  to  $\approx 5 \mu\text{m}$  deep (Figure 5A,B). The EDS showed these rings to be significantly depleted in Na and K (Figure 5C). The rings coincide with the presence of surface organics for many of the samples. No chemical link has yet been made between these observations.

The dark glass, which is in close spatial proximity to the clear glass on the sectioned sample and was likely exposed to the same or similar external alteration conditions, contained some crystalline phases (magnetite and quartz), and an amorphous phase (Figure 3D). The SEM images of the surface of the glass showed some pitting, which was not present on the clear glass. Like the clear glass, the surface of the dark glass had intermittent coverage by organic material.

## 5 | DISCUSSION

### 5.1 | Chemical composition of clear glass

The major elemental constituents of the clear glass are Na, K, Al, and Si. The high concentration of K in the glass



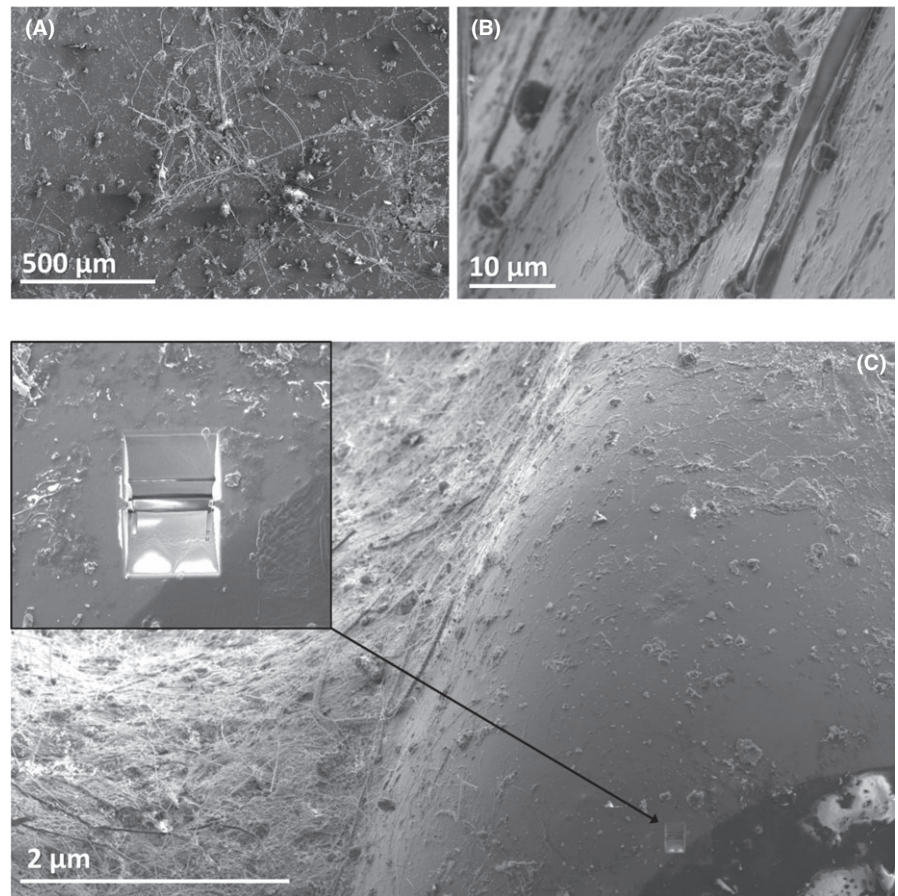


**FIGURE 4** Secondary electron images of the clear glass surface on the Broborg sample (A and B) showing variety of organic material. C shows the clear glass surface and the area from which the FIB section was taken (inset showing FIB section)

**TABLE 2** Elemental concentration, expressed as oxides, of Hillfort clear glass determined by  $\mu$ XRF, with measured values are reported in wt% and normalized to 100. Comparison data from by Kresten et al.<sup>36</sup> as measured by Electron Probe Microanalysis (EPMA); others determined by simple difference. For comparison purposes, all Fe data has been converted to  $\text{Fe}_2\text{O}_3$  and implies composition only and not redox state. Also shown are typical low activity waste (LAW) glass and natural basaltic glass compositions, to compare with the Hillfort clear and dark glasses, respectively. Quantification of spectra at specific locations was performed with peak to peak ratios, in lieu of elemental standards, following the procedure described by Shen et al.<sup>38</sup> This data was collected and analyzed at Pacific Northwest National Laboratory

Oxide (wt%)	Clear glass - $\mu$ XRF (this work)	Clear glass <sup>30</sup>	LAW-A-44 glass <sup>62</sup>	Dark glass - $\mu$ XRF (this work)	Dark glass <sup>30</sup>	Typical basaltic glass <sup>63</sup>
$\text{Na}_2\text{O}$	4.71	5.8	20.00	4.76	2.8	4.5
$\text{MgO}$	1.18	0.26	1.99	2.69	6.2	6.7
$\text{Al}_2\text{O}_3$	15.12	22.1	6.20	14.19	16.5	11.7
$\text{SiO}_2$	67.37	61.7	44.55	48.95	51.1	50.7
$\text{P}_2\text{O}_5$	1.41	0.24	0.03	1.98	0.27	0
$\text{K}_2\text{O}$	8.94	5.9	0.50	2.39	1.3	0.7
$\text{CaO}$	0.22	1.40	1.99	11.33	9.8	10.6
$\text{TiO}_2$	0.15	0.12	1.99	1.63	0.85	1.9
$\text{MnO}$	0.02	0.0	0	0.34	0.25	0.4
$\text{Fe}_2\text{O}_3$	0.91	1.11	6.98	11.75	10.44	13.1
$\text{B}_2\text{O}_3$	0	0	8.90	0	0	0
Others	0	1.37	6.87	0	0.49	0
Total	100	100	100	100	100	100

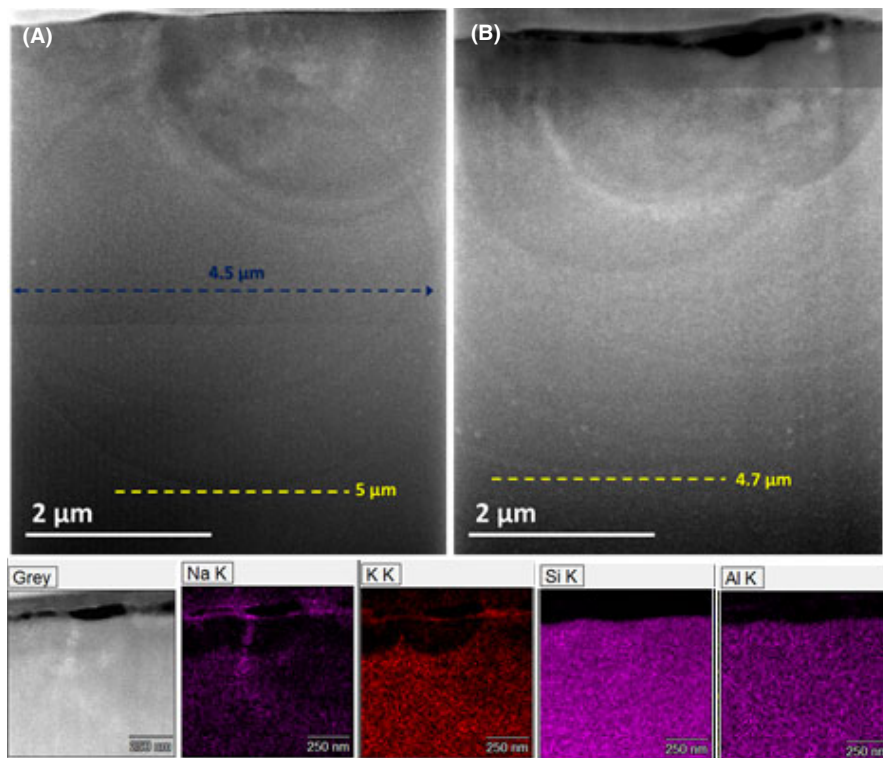


**FIGURE 5** Bright-field STEM images (A-B) of FIB cross-section removed from clear glass surface (as shown in Figure 4C). Hemispherical structures in 3D appear semicircular in cross section, and indicate alteration occurred in multiple locations and extend up to 5 μm into the glass. EDS analysis of these sections (C) shows evidence of alkali depletion within these semicircle regions

could be attributed to the use of a wood charcoal melt method, a theory in accordance with previous work.<sup>30</sup> Wood ash and charcoals tend to have high concentrations of K (a few to 10s of wt%), and can produce alkali and alkaline earth carbonates at the temperatures reported for the firing of Broborg.<sup>39</sup> These carbonates could have been an available source of K during the vitrification of the wall. The large concentrations of Si and Al in the clear glass can be ascribed to their source material(s), which may have been the mixed quartz and feldspar portions of the granite gneiss. If amphibolite, or some iron-rich constituent of the granite gneiss had been the main sources of the Si or Al then the Fe concentration in the clear glass would have been elevated. It is unlikely that the clear glass was produced from a singular melt of the pure quartz phases in the gneiss as the predicted melting temperature of the hillfort glass,  $\approx 1130^{\circ}\text{C}$ ,<sup>30</sup> which is too low to soften pure, crystalline quartz melting point of  $\approx 1670^{\circ}\text{C}$  for  $\beta$  tridymite, and  $\approx 1713^{\circ}\text{C}$  for  $\beta$  cristobalite.<sup>40</sup> It is probable that the clear glass formed when the quartz mixed with potassium flux from the organic fuel, or with potassium feldspar. Research into the co-melting of potassium feldspar with quartz has shown that a eutectic point can be reached at  $1150^{\circ}\text{C}$ , which is the predicted glass melting temperature for the glasses found at the Broborg Site.<sup>28,30,41</sup> This temperature is significantly lower than that for melting pure potassium silicate glasses, which has been reported by Scherer and Uhlmann as  $>1400^{\circ}\text{C}$ .<sup>42</sup> However, the role of water and fugitive volatile elements (eg, F, Cl) in lowering

the melting temperature or melt viscosity cannot be discounted. The effect of water on glass melting has been previously documented for silicate glasses,<sup>43,44</sup> and is well known to play a factor in amphibolite melting temperatures.<sup>45</sup>

The presence of other elements in the clear glass, those which are not accounted for by the melting of quartz and potassium feldspar, could be attributed to the presence of mica with a relatively low Fe content (eg, muscovite). This mineral has been identified in the granite gneiss used to build the fortified wall.<sup>30</sup> It has been proposed in studies of Scottish hillforts that low temperature melting ( $800\text{--}950^{\circ}\text{C}$ ) occurred due to decomposition of mica (such as biotite) and reaction with quartz to produce potassium feldspars, orthopyroxenes, and liquid.<sup>46-48</sup> Alternatively, these lower quantity elements could have been sourced from molten amphibolite following a scenario previous discussed by Sjöblom et al.<sup>21</sup>

## 5.2 | Chemical composition of dark glass

In contrast to the clear glass, chemistry of the dark glass is higher in Fe (as  $\text{Fe}_2\text{O}_3$ ; 0.91 wt%, clear glass vs 11.75 wt%, dark glass), alkaline earths (CaO; 0.22 wt%, clear glass vs 11.33 wt%, dark glass), transition metals ( $\text{TiO}_2$ , 0.15 wt%, clear glass vs 1.63 wt%, dark glass), and lower in alkali earths ( $\text{K}_2\text{O}$ ; 8.94 wt%, clear glass vs 2.39 wt%, dark glass) and Si ( $\text{SiO}_2$ ; 67.37 wt%, clear glass vs 48.95 wt%, dark glass). The chemistry of the dark glass

similar to that found in some basaltic glasses.<sup>49</sup> The glass was found to contain crystalline phases related to those found in amphibolite. To confirm this observation, chemical and mineralogical analyses of metamorphic mafic-intermediate rocks from outcrops near Broborg samples were conducted.<sup>50</sup> These samples contained varying proportions of hornblende (amphibole), chlorites (possibly altered mica), oligoclase, plagioclase (albite and anorthite), and quartz. It has been suggested that the dark glass is the result of an amphibolite melt, and formed when the amphibolite was exposed to the same melt temperature as the granite.<sup>30,36</sup> It is plausible that the amphiboles decomposed to anhydrous minerals, mainly pyroxenes (eg, diopside) at the elevated temperatures of the melt, and the feldspar phases melted (liquidus temperature of albite is 1118°C)<sup>51</sup> into the dark glass. The temperature of melting for these phases may have been even lower if water was present. Research is ongoing to understand the melting behavior of amphibolite in hydrated and dehydrated states to determine the original melting conditions utilized.

### 5.3 | Factors affecting alteration of glass surfaces

Both glasses show evidence of surface alteration. However, the extent and character of alteration is not the same for the 2 glasses, and the dissimilarity could be related to differences in their glass compositions. The formation of semicircular alteration patterns on a micron scale at the clear glass surface (shown in Figure 5) may be an indication of microbially induced alteration. Semicircle alteration patterns as the result of microbe-induced alteration have been observed previously in volcanic glass.<sup>52</sup> However, the textural and chemical evidence for bio-alteration of glass at Broborg must also be carefully evaluated with other abiotic processes that can affect silicate glasses alteration. It is most likely that multiple mechanisms, abiotically and biotically driven, are responsible for alteration of the glasses. Such mechanisms could be related to the metabolic processes of biological species on the glass surface, water recharge rate, aqueous chemistry at the hillfort, and chemistry of the soil matter in contact with the glass.

The influence of microbes on glass alteration rates and mechanisms is of particular interest as microbes have been known to play a role in glass alteration in natural environments,<sup>52-56</sup> but they have been relatively understudied in the context of the durability of nuclear waste glasses being designed for disposal at the Hanford Site.<sup>53,55</sup> This sentiment has been previously stated by Donald, who noted that complexing organic acids, as produced by some microorganisms, can have a significant (positive and/or negative)

altering effect on waste glasses.<sup>57</sup> More research is needed to understand the overall influence of microbes on long-term glass alteration given the lack of published data on this matter.<sup>57</sup> To date, only a limited number of short-term laboratory tests have been conducted on a low level waste glass (LAWA44) with microbial strains native to the Hanford Site, and the results of these experiments were inconclusive.<sup>22</sup>

Identification of microbes in near-surface/surface environments at Broborg is necessary to determine the metabolic processes that may be active on the glass surfaces and their by-products. Comparisons can then be made with microbes present in the near surface at the Hanford Site. Classification of biologically mediated by-products is important as some are crystalline and may be similar to those formed when glass is altered under abiotic conditions, thus, presenting a challenge for identification of the dominant and/or competing alteration mechanism.<sup>58-60</sup>

Knowing which species are present on the glass provides information on the approximate pH of the altering solution(s). Different classes of organisms will regulate the pH of their environments to develop a more habitable surface upon which to live.<sup>58,61</sup> For example, phototrophs, organisms that biologically respond to light, can increase the pH of a contact solution to above 10, a pH level that can lead to a significant increase in the rate of glass alteration.<sup>58</sup> Other organisms have been recorded to drive the pH > 5;<sup>62</sup> which can also increase the glass alteration rate if oxalic acid, a common bio-acid found in natural environments, is present in solution.<sup>63</sup> In addition, recent work by Jantzen and co-workers has shown that leachant pH plays an important role in the formation of secondary (ie, crystalline) alteration phases from alumino-silicate hydrogels.<sup>64</sup> When excess hydroxide anions and alkali are present in the leachant the hydrogel will mineralize to zeolites. This formation of zeolites has been linked to the resumption of glass dissolution, and an increase in the extent to which a glass may be altered, a theory that was first proposed by Iseghem and Grambow in 1987.<sup>65,66</sup>

Fresh samples from the Broborg site are needed to accurately characterize the biosphere surrounding the hillfort glasses. An excavation of Broborg is planned to obtain vitrified material, groundwater samples, and soil cores for chemical and microbial characterization. DNA extraction from the samples followed by quantitative polymerase chain reaction (qPCR) will allow the comparison of fungal biomass relative to bacteria biomass, both associated with the glass and in the surrounding soil. DNA sequencing can then be used to analyze the composition and diversity of the bacterial and fungal communities present. This information will be used in context of weather cycle<sup>35</sup> and vegetative growth<sup>31</sup> data collected for or near to the site.



## 5.4 | Use of clear glass as a long-term analogue for Hanford LAW glass

A case can be made for using the Broborg clear glass as a possible analogue for Hanford LAW glasses. The clear glass is of a chemical composition similar to the LAW glasses (Table 2),<sup>49</sup> it shows physical and chemical indications of alteration (Figure 5), it has been altered under conditions similar to those expected for the disposal of the LAW glasses (ie, near-surface, in contact with soil, and with seasonal exposure to natural waters), and, with the excavation of fresh samples from Broborg, will come from known provenance. In addition, information about the altering environment over the course of the glass's exposure time can be found in the literature. One oxide not identified in the Broborg glasses, but present in LAW glasses at levels between  $\approx 4$  wt% to  $\approx 15$  wt%, is  $B_2O_3$ .<sup>1</sup> There is no published evidence that the Broborg glasses contain consequential amounts of B, nor is it to be expected as the minerals involved in the vitrification do not contain significant B concentrations. However, and as already stated, a glass does not need to contain B to be considered as an analogue for nuclear waste glasses. Therefore, the clear glass from Broborg meets the criteria for an analogue, and therefore could possibly be used with other analogue glasses to test the predictive capability of geochemical models to simulate long-term alteration (over 1500 years) of LAW glass in a near surface disposal facility. Other analogue glasses, with different compositions, should be used in conjunction with the Broborg clear glass to provide additional confidence in any glass alteration model's ability to predict the long-term durability of nuclear waste glasses. Such additional analogue glasses could be those that contain higher levels of B, such as borosilicate glass artifacts buried in near-surface conditions, though these would be of significantly younger ages.

The dark glass is not sufficiently chemically similar to the LAW glasses (due to a lack of alkali), and does not meet the criteria for a LAW glass analogue. It should be pointed out that the dark glass is very similar to basaltic glass, long considered by the community as a nuclear waste glass analogue.<sup>67</sup> However, the dark glass and clear glass were altered in the same environment. Therefore, comparison of how the 2 glasses altered at Broborg can provide invaluable information on how glass chemistry affects glass alteration in natural environments.

## 5.5 | Insight into ancient vitrification methods

Data collected from the specimen also provided some understanding into the melting techniques used by the ancient builders in the construction of Broborg. Most of

the minerals that were vitrified at Broborg, as identified by this and previous studies,<sup>30,36</sup> have higher melting points than could have been easily achieved by the ancient people. Therefore, special techniques to lower the melting point of the minerals or achieve higher temperatures were most likely implemented. Previous studies have suggested that the use of forced air heating, either by natural draught or bellows, could have been used to achieve the high temperatures.<sup>68,69</sup> The hydrated state of the minerals in the amphibolite and the presence of water in the fuel source may also have lowered the melting temperature.<sup>30</sup> Further experimental work on rock melting is underway to clarify these conditions.

## 6 | CONCLUSION

Glasses found on artifacts recovered from the Broborg site in Sweden are currently under study. The presence of 2 glasses—clear and dark—has been reconfirmed in the samples, and a careful sampling methodology for the analysis of the glasses has been detailed. Based on data collected with  $\mu$ XRD and  $\mu$ XRF, and preliminary knowledge of the melting conditions at the site, it has been proposed that the clear, purely amorphous glass was possibly formed due the melting of quartz with potassium flux- originating most likely from potassium feldspar in the granitic gneiss. Low-Fe micas, eg, muscovite, may have been incorporated into the melt, resulting in the low concentrations of Fe identified in the clear glass by  $\mu$ XRF. These results are consistent with previous findings of Kresten et al.<sup>30</sup>

Due to similarities in chemical composition, presence of chemical and physical features consistent with an alteration layer, and exposure to near-surface weather cycles, the Broborg clear glass meets the criteria for study as a long-term alteration analogue for Hanford Low Activity Waste glasses. The dark glass, although different enough chemically from LAW glasses, can provide important contextual information on how glasses with dissimilar compositional chemistries alter when exposed to the same environment. Additional research is needed to understand how the diverse alteration textures and chemistries detected on the 2 glasses were formed. Ultimately, knowledge of alteration mechanisms, obtained through characterization of the Broborg hillfort glasses, will inform models for predicting glass durability that are to be used in performance assessments and environmental impact statements for radioactive waste disposal facilities.

## ACKNOWLEDGMENTS

The authors thank Professor Peter Kresten for sharing his knowledge and for consenting to part from a large fraction

of his samples that had been collected during many years of work. The authors also wish to recognize the Jim Henle, Anthony Guzman and Clyde Chamberlin (PNNL) for performing the rock section and George Zhang (PNNL) for assistance with Figure 2. The project has been financed by United States Department of Energy Office of Environmental Management, International Programs through its Office of River Protection. A portion of this research was performed at the Environmental Molecular Sciences Laboratory (EMSL), a DOE Office of Science User Facility sponsored by the Office of Biological and Environmental Research and located at Pacific Northwest National Laboratory under proposal number 49141. Certain commercial products are identified in this paper to specify the experimental procedures in adequate detail. This identification does not imply recommendation or endorsement by the authors or by the National Institute of Standards and Technology or Department of Energy, nor does it imply that the products identified are necessarily the best available for the purpose. Contributions of the Department of Energy and National Institute of Standards and Technology are not subject to copyright.

## ORCID

Jamie L. Weaver  <http://orcid.org/0000-0002-6762-0568>

John S. McCloy  <http://orcid.org/0000-0001-7476-7771>

Tamas Varga  <http://orcid.org/0000-0002-5492-866X>

## REFERENCES

- Vienna JD, Ryan JV, Gin S, Inagaki Y. Current understanding and remaining challenges in modeling long-term degradation of borosilicate nuclear waste glasses. *Int J Appl Glass Sci.* 2013;4:283-294.
- Jantzen CM, Brown KG, Pickett JB. Durable glass for thousands of years. *Int J Appl Glass Sci.* 2010;1:38-62.
- Weaver JL, McCloy JS, Ryan JV, Kruger AA. Ensuring longevity: ancient glasses help predict durability of vitrified nuclear waste. *Am Ceram Soc Bull.* 2016;95:18-23.
- Ewing RC, Jercinovic MJ, eds. Natural Analogues: Their Application to the Prediction of the Long-Term Behavior of Nuclear Waste Forms. MRS Proceedings. Cambridge, UK: Cambridge Univ Press; 1986.
- Lutze W, Grambow B, Ewing RC, Jercinovic MJ. The use of natural analogues in the long-term extrapolation of glass corrosion processes. In: Côme B, Chapman NA, eds. Natural Analogues in Radioactive Waste Disposal. Dordrecht: Springer; 1987:142-152.
- Jantzen C, Plodinec M. Prediction of nuclear waste glass durability from natural analogs. *J Non-Cryst Solids.* 1984;67:207-223.
- Jantzen CM. Prediction of nuclear waste glass durability from natural analogs. In: Passchier WF, Bosnjakovic BFM, eds. International Symposium on Ceramics in Nuclear Waste Management, Chicago, IL, USA. Westerville, OK, USA: American Ceramic Society Inc; 1986:703-712.
- Ewing R. Natural glasses: analogues for radioactive waste forms. In: McCarthy G, ed. Scientific Basis for Nuclear Waste Management. New York, NY: Plenum Press; 1979:57-68.
- Miller W, Alexander R, Chapman N, McKinley JC, Smellie J. Geological Disposal of Radioactive Wastes and Natural Analogues. Oxford, UK: Elsevier; 2000.
- Verney-Carron A, Gin S, Libourel G. A fractured roman glass block altered for 1800 years in seawater: analogy with nuclear waste glass in a deep geological repository. *Geochim Cosmochim Acta.* 2008;72:5372-5385.
- Ebert WL. The Effects of the Glass Surface Area/Solution Volume Ratio on Glass Corrosion: A Critical Review. Lemont, IL: Argonne National Laboratory; 1995.
- Grambow B, Jercinovic M, Ewing R, Byers C, eds. Weathered Basalt Glass: A Natural Analogue for the Effects of Reaction Progress on Nuclear Waste Glass Alteration. MRS Proceedings. Cambridge, UK: Cambridge Univ Press; 1985.
- Lombardo T, Gentaz L, Verney-Carron A, et al. Characterisation of complex alteration layers in medieval glasses. *Corros Sci.* 2013;72:10-19.
- Strachan DM, Crum JV, Ryan JV, Silvestri A. Characterization and modeling of the cemented sediment surrounding the Iulia Felix glass. *Appl Geochem.* 2014;41:107-114.
- Verney-Carron A, Gin S, Frugier P, Libourel G. Long-term modeling of alteration-transport coupling: application to a fractured Roman glass. *Geochim Cosmochim Acta.* 2010;74:2291-2315.
- Verney-Carron A, Gin S, Libourel G. Archaeological analogs and the future of nuclear waste glass. *J Nucl Mater.* 2010;406:365-370.
- Macfarlane A, Martin G. Glass: A World History. Chicago, IL: University of Chicago Press; 2002.
- Konijnendijk WL, Stevels JM. The structure of borate glasses studied by Raman scattering. *J Non-Cryst Solids.* 1975;18:307-331.
- Bunker BC, Arnold GW, Day DE, Bray P. The effect of molecular structure on borosilicate glass leaching. *J Non-Cryst Solids.* 1986;87:226-253.
- Sjöblom R, Ecke H, Brännvall E, eds. On the possibility of using vitrified forts as anthropogenic analogues for assessment of long-term behaviour of vitrified waste. In: Popov V, Itoh H, Brebbia CA, eds. International Conference on Waste Management and the Environment VI; New Forest, UK. Southampton, Boston: WIT Press; 2012:225-236.
- Sjöblom R, Weaver J, Peeler D, et al. eds. Vitrified hillforts as anthropogenic analogues for nuclear waste glasses: project planning and initiation. *Int J Sust Develop Plann.* 2016;11:897-906.
- Pierce EM, McGrail BP, Rodriguez EA, et al. Waste form release data package for the 2005 integrated disposal facility performance assessment. PNNL-14805, Richland, WA: Pacific Northwest National Laboratory; 2004.
- McIntosh J. Handbook to Life in Prehistoric Europe. New York: Oxford University Press on Demand; 2009.
- Schnittger B. Östergötlands Fornborgar. Meddelanden från Östergötlands fornminnesförening; 1909: 14-17.
- Hermelin E. Om Södermanlands fornborgar; 1929.
- Olausson M. At peace with walls-Fortifications and their significance AD 400-1100. In: Olausson L, Olausson M, eds. The Martial Society Aspects of Warriors, Fortifications and Social Change in Scandinavia, B. Stockholm, Sweden: Stockholm University; 2009:35-70.

27. Wall Å. Borderline viewpoints: the early iron age landscapes of hanged mountains. *Curr Swedish Archeol.* 2002;10:95-114.
28. Kresten P, Goedicke C, Manzano A. TL-dating of vitrified material. *Geochronometria.* 2003;22:9-14.
29. Youngblood E, Fredriksson B, Kraut F, Fredriksson K. Celtic vitrified forts: implications of a chemical-petrological study of glasses and source rocks. *J Archaeol Sci.* 1978;5:99-121.
30. Kresten P, Kero L, Chyessler J. Geology of the vitrified hill-fort Broborg in Uppland, Sweden. *GFF.* 1993;115:13-24.
31. Mokhonko Y. Vegetation changes and human impact around Runsa hillfort as interpreted from a sedimentary record in Lake Mälaren. Masters thesis Physical Geography and Quarternary Geology. Stockholms University, Stockholm, Sweden; 2011.
32. MacDonald G, Bennett K, Jackson S, et al. Impacts of climate change on species, populations and communities: palaeobiogeographical insights and frontiers. *Prog Phys Geogr.* 2008;32:139-172.
33. Parducci L, Matetovici I, Fontana SL, et al. Molecular-and pollen-based vegetation analysis in lake sediments from central Scandinavia. *Mol Ecol.* 2013;22:3511-3524.
34. Bergström H, Moberg A. Daily air temperature and pressure series for Uppsala (1722–1998). In: Camuffo D, Jones P, eds. Improved Understanding of Past Climatic Variability from Early Daily European Instrumental Sources. Dordrecht: Springer; 2002:213-252.
35. Moberg A, Sonechkin DM, Holmgren K, Datsenko NM, Karlén W. Highly variable Northern Hemisphere temperatures reconstructed from low-and high-resolution proxy data. *Nature.* 2005;433:613-617.
36. Kresten P, Ambrosiani B. Swedish vitrified forts-a reconnaissance study. *Fornvännen.* 1992;87:1-17.
37. Deer W, Howie R, Zussman J, eds. Rock-forming Minerals, 2B, Double-Chain Silicates. London: Geological Society; 1997.
38. Shen R, Russ J. A simplified fundamental parameters method for quantitative energy-dispersive X-ray fluorescence analysis. *X-Ray Spectrom.* 1977;6:56-61.
39. Misra MK, Ragland KW, Baker AJ. Wood ash composition as a function of furnace temperature. *Biomass Bioenerg.* 1993;4:103-116.
40. Deer WA, Howie RA, Zussman J. An Introduction to the Rock-Forming Minerals. London, UK: Longman; 1992.
41. Reifenstein A, Kahraman H, Coin C, Calos N, Miller G, Uwins P. Behaviour of selected minerals in an improved ash fusion test: quartz, potassium feldspar, sodium feldspar, kaolinite, illite, calcite, dolomite, siderite, pyrite and apatite. *Fuel.* 1999;78:1449-1461.
42. Scherer G, Uhlmann DR. Diffusion-controlled crystal growth in K<sub>2</sub>O SiO<sub>2</sub> compositions. *J Non-Cryst Solids.* 1977;23:59-80.
43. Shelby J, McVay G. Influence of water on the viscosity and thermal expansion of sodium trisilicate glasses. *J Non-Cryst Solids.* 1976;20:439-449.
44. Hetherington G, Jack K, Kennedy J. The viscosity of vitreous silica. *Phys Chem Glasses.* 1964;5:130-136.
45. Beard JS, Lofgren GE. Dehydration melting and water-saturated melting of basaltic and andesitic greenstones and amphibolites at 1, 3, and 6.9 kb. *J Petrol.* 1991;32:365-401.
46. Friend C, Charnley N, Clyne H, Dye J. Experimentally produced glass compared with that occurring at The Torr, NW Scotland, UK: vitrification through biotite melting. *J Archaeol Sci.* 2008;35:3130-3143.
47. Friend C, Dye J, Fowler M. New field and geochemical evidence from vitrified forts in South Morar and Moidart, NW Scotland: further insight into melting and the process of vitrification. *J Archaeol Sci.* 2007;34:1685-1701.
48. Friend CR, Kirby JE, Charnley NR, Dye J. New field, analytical data and melting temperature determinations from three vitrified forts in Lochaber, Western Highlands, Scotland. *J Archaeol Sci Rep.* 2016;10:237-252.
49. Bates JK, Bradley CR. High-level Waste Borosilicate Glass: A Compendium of Corrosion Characteristics, vol. 2. Washington: USDOE; 1994. Contract No.: DOE/EM-0177-Vol 2.
50. Ogenhall E. Amphibolitic rocks near Broborg, Uppland: Chemical and mineralogical analyses of metamorphic mafic-intermediate rocks from outcrops near the pre-historic vitrified hillfort Broborg and a boulder in the hillfort. Field and Sample Analysis ReportArkeologerna, Statens Historiska Museer, Uppsala, Sweden; 2016. Contract No.: 5.1.1-01422-2015.
51. Johannes W, Holtz F. Petrogenesis and Experimental Petrology of Granitic Rocks. Berlin: Springer Science & Business Media; 2012.
52. Staudigel H, Furnes H, McLoughlin N, Banerjee NR, Connell LB, Templeton A. 3.5 billion years of glass bioalteration: volcanic rocks as a basis for microbial life? *Earth Sci Rev.* 2008;89:156-176.
53. Koestler RJ, Santoro ED, Ransick L, Brill RH, Lynn M. Preliminary scanning electron microscopy study of microbiologically induced deterioration of high alkali low-lime glass. *Biodeterior Res.* 1987;1:295-307.
54. Aouad G, Crovisier J-L, Geoffroy V, Meyer J-M, Stille P. Microbially-mediated glass dissolution and sorption of metals by *Pseudomonas aeruginosa* cells and biofilm. *J Hazard Mater.* 2006;136:889-895.
55. Piñar G, Garcia-Valles M, Gimeno-Torrente D, Fernandez-Turiel JL, Etenauer J, Sterflinger K. Microscopic, chemical, and molecular-biological investigation of the decayed medieval stained window glasses of two Catalonian churches. *Int Biodeterior Biodegradation.* 2013;84:388-400.
56. Fisk MR, Crovisier J-L, Honnorez J. Experimental abiotic alteration of igneous and manufactured glasses. *CR Geosci.* 2013;345:176-184.
57. Donald IW. Waste Immobilization in Glass and Ceramic Based Hosts: Radioactive, Toxic and Hazardous Wastes. Chichester, UK: John Wiley & Sons; 2010.
58. Krumbein WE, Urzi CE, Gehrman C. Biocorrosion and biodeterioration of antique and medieval glass. *Geomicrobiol J.* 1991;9:139-160.
59. Perez A, Rossano S, Trcera N, et al. Impact of iron chelators on short-term dissolution of basaltic glass. *Geochim Cosmochim Acta.* 2015;162:83-98.
60. Garcia-Valles M, Gimeno-Torrente D, Martínez-Manent S, Fernández-Turiel J. Medieval stained glass in a Mediterranean climate: typology, weathering and glass decay, and associated biomineralization processes and products. *Am Miner.* 2003;88:1996-2006.
61. Thorseth I, Furnes H, Tumyr O. Textural and chemical effects of bacterial activity on basaltic glass: an experimental approach. *Chem Geol.* 1995;119:139-160.
62. Bosecker K. Bioleaching: metal solubilization by microorganisms. *FEMS Microbiol Rev.* 1997;20:591-604.
63. Oelkers EH, Gislason SR. The mechanism, rates and consequences of basaltic glass dissolution: I. An experimental study of



- the dissolution rates of basaltic glass as a function of aqueous Al, Si and oxalic acid concentration at 25°C and pH = 3 and 11. *Geochim Cosmochim Acta*. 2001;65:3671-3681.
64. Jantzen CM, Trivelpiece CL, Crawford CL, Pareizs JM, Pickett JB. Accelerated leach testing of glass (ALTGLASS): II. Mineralization of hydrogels by leachate strong bases. *Int J Appl Glass Sci*. 2017;8:84-96.
65. Ribet S, Gin S. Role of neoformed phases on the mechanisms controlling the resumption of SON68 glass alteration in alkaline media. *J Nucl Mater*. 2004;324:152-164.
66. Van IP, Grambow B. The long-term corrosion and modelling of two simulated Belgian reference high-level waste glasses. MRS Online Proceedings Library Archive. 1987: 112.
67. Crovisier J-L, Advocat T, Dussossoy J-L. Nature and role of natural alteration gels formed on the surface of ancient volcanic glasses (Natural analogs of waste containment glasses). *J Nucl Mater*. 2003;321:91-109.
68. Childe VG, Thorneycroft W. The experimental production of the phenomena distinctive of vitrified forts. 1938.
69. Childe VG, Thorneycroft W. The vitrified fort at rahoy, Morvern, Argyll; 1938.

**How to cite this article:** Weaver JL, Pearce CI, Sjöblom R, et al. Pre-viking Swedish hillfort glass: A prospective long-term alteration analogue for vitrified nuclear waste. *Int J Appl Glass Sci*. 2018;00:1–15. <https://doi.org/10.1111/ijag.12351>